The synthesis and biological applications of photo-activated ruthenium anticancer drugs

Lameijer, L.N.

Chapter 4: Photodynamic therapy or photoactivated chemotherapy?

Effects of the bidentate ligand on the photophysical properties, cellular uptake, and (photo)cytotoxicity of glycoconjugates based upon the $[Ru(tpy)(NN)(L)]^{2+}$ scaffold

Abstract: Ruthenium polypyridyl complexes have received widespread attention as potential chemotherapeutics in photodynamic therapy (PDT) and in photochemotherapy (PACT). Herein we investigate a series of sixteen ruthenium polypyridyl complexes with general formula $[Ru(tpy)(N\text{-}N)(L)]^{+/2+}$ (tpy = 2,2':6',2''-terpyridine, N-N = bpy (2,2'-bipyridine), phen (1,10-phenanthroline), dpq (pyrazino[2,3-*f*][1,10]phenanthroline), dppz (dipyrido[3,2-*α*:2',3'-*c*]phenazine, dppn (benzo[*i*]dipyrido[3,2-*α*:2',3'-*c*]phenazine), pmip (2-(4-methyl-phen-yl)-1*H*-imidazo[4,5-*f*][1,10]phenanthroline), pymi ((*E*)-*N*-phenyl-1-(pyridin-2-yl)methanimine), or azpy (2-(phenylazo)pyridine), L = Cl or 2-(2-(2-(methylthio)ethoxy)ethoxy)ethyl-β-D-glucopyranoside) and their potential for either PDT or PACT. We demonstrate that although increased lipophilicity is generally related to increased uptake of these complexes, it does not necessarily lead to increased (photo)cytotoxicity. However, the non-toxic complexes are excellent candidates as PACT carriers.

This chapter will be submitted for publication: L. N. Lameijer, T. G. Brevé, V. H. S. van Rixel, S. H. C. Askes, M. Siegler, S. Bonnet.; *Manuscript in preparation.*

4.1 Introduction

Ruthenium based anti-cancer compounds have been investigated for several decades[1] as potential alternatives to the clinically approved cisplatin. Cisplatin is associated with serious side effects such as renal toxicity, neurotoxicity, and hearing loss.[2] The most thoroughly investigated ruthenium-based anti-cancer agents, NAMI-A and KP1019, both reached phase II clinical trials before being abandoned.[3] More recently the tunable photophysical properties of ruthenium(II) polypyridyl complexes have been used to develop compounds combating bacterial resistance to antibiotics,[4] or new photosensitizers for photodynamic therapy as an alternative to *e.g.* Photofrin.[5] Recently, the group of McFarland have made a great step forward in this field, by entering Phase I clinical trials with a Ru(II)-thiophene-polypyridyl-based photosensitizer, TLD1433.[6] Simultaneously, a great interest has been shown in the development of sterically strained ruthenium(II) complexes for the light-induced delivery of cytotoxic cargo.[7] This last approach is often referred to as photo-activated chemotherapy (PACT).[3b] The proof-of-concept for ruthenium-based PACT was first demonstrated by Etchenique's group, who showed that the photoinduced release of the potassium channel blocker 4-aminopyridine (4AP) from $[Ru(bpy)_2(4AP)_2]^{2+}$ upon visible light irradiation, lead to a response in leech neurons.[8] Many other examples of ruthenium complexes used as photoactive agents releasing anticancer molecules have been developed by the group of Turro,[9] Gasser,[10] Glazer,[11] Kodanko[12], and Bonnet.[13] Following up on our initial work using thioether monodentate ligands to cage cytotoxic aqua ruthenium complexes,[13-14] we herein report a series of related chloride complexes [**1a**]Cl-[**8a**]Cl having the general formula [Ru(tpy)(N-N)(Cl)]Cl with N-N = bpy (2,2'-bipyridine), phen (1,10-phenanthroline), dpq (pyrazino[2,3-*f*][1,10]phenanthroline), dppz (dipyrido[3,2-*a*:2',3'-*c*]phenazine, dppn (benzo[*i*]dipyrido[3,2-*a*:2',3'-*c*]phenazine), pmip (2-(4-methyl-phen-yl)-1*H*-imidazo[4,5-*f*][1,10]phenanthroline), pymi ((*E*)-*N*-phenyl-1-(pyridin-2-yl)methanimine), or azpy (2-(phenylazo)pyridine), respectively, and of their water-soluble derivatives [Ru(tpy)(N-N)(L)]$(PF_6)_2$ ([**1b**]$(PF_6)_2$-[**8b**]$(PF_6)_2$), where R = (2-(2-(2-(methylthio)ethoxy)ethoxy)ethyl-β-D-glucopyranoside is a thioether-glucose conjugate (Figure 4.1).

On the one hand, [Ru(tpy)(bpy)(Cl)]Cl is known to be poorly cytotoxic to cancer cells.[15] On the other hand, we recently demonstrated that [Ru(tpy)(dppn)(L)]$(PF_6)_2$ ([**5b**]$(PF_6)_2$, (Figure 4.1) has unique phototoxic properties based on a dual mode-of-action involving both photosubstitution of the thioether ligand and singlet oxygen generation. In this chapter, we compare the photophysical properties of all conjugates [**1b**]$(PF_6)_2$-[**8b**]$(PF_6)_2$ and of their chloride analogues [**1a**]Cl-[**8a**]Cl in water, and correlate them to the uptake and cytotoxicity in cancer cells. Critically, the glucose-containing ligand L ensures that all thioether-ruthenium complexes are soluble in water, allowing their photochemistry to be studied independently from the lipophilicity of the N-N spectator bidentate ligand.

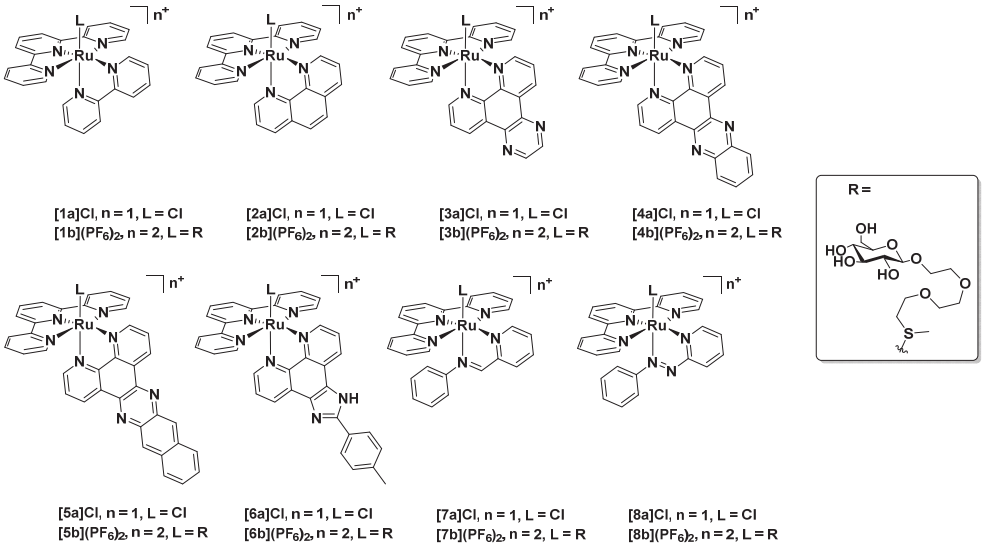

Figure 4.1. Chemical structure of the complexes used in this study. General formula $[Ru(tpy)(N\text{-}N)(L)]^{n+}$, N-N = bpy, phen, dpq, dppz, dppn, pmip, pymi or azpy. L = Cl or L = R (2-(2-(2-(methylthio)ethoxy)ethoxy)ethyl-β-D-glucopyranoside).

4.2 Results

4.2.1 Synthesis

Chloride complexes [**1a**]Cl,[16] [**2a**],Cl[17] [**4a**]Cl,[18] [**5a**]Cl,[13b] [**7a**]Cl,[19] [**8a**]Cl,[20] and the ligand 2-(2-(2-(methylthio)ethoxy)ethoxy)ethyl-β-D-glucopyranoside (**R**)[13b] were synthesized as reported previously. Complex [**1b**]$(PF_6)_2$ was synthesized as described in Chapter 2. Complexes [**3a**]Cl and [**6a**]Cl were synthesized by reacting $[Ru(tpy)Cl_3]$ with the bidentate ligand dpq or pmip in the presence of triethylamine as a reducing agent. The chloride complexes [**2a**]Cl-[**8a**]Cl were then reacted with an excess of the thioether ligand **R** in the dark in water. Silica column purification of the crude complexes, followed by size exclusion chromatography, afforded the thioether-glucose ruthenium conjugates [**2b**]$(PF_6)_2$ and [**4b**]$(PF_6)_2$ as orange and red solids and [**8b**]$(PF_6)_2$ as a purple solid. To ease purification of the pmip complex [**6b**]$(PF_6)_2$ the synthesis was carried out similarly to the previously reported synthesis of [**5b**]$(PF_6)_2$[13b] by first converting the chloride precursor [**5a**]Cl to the aqua species $[Ru(tpy)(pmip)(H_2O)](NO_3)_2$ using $AgNO_3$, followed by reaction of the thioether ligand with the aqua complex. Similarly, the syntheses of [**3b**]$(PF_6)_2$ and [**7b**]$(PF_6)_2$ were carried out in the presence of $AgPF_6$ to ensure *in situ* conversion to the aqua species. All chloride complexes except [**4a**]Cl, [**5a**]Cl and [**6a**]Cl and all thioether complexes are soluble in water. As reported for the complex $[Ru(tpy)(bpy)(Hmte)](PF_6)_2$,[21] all thioether complexes showed an upfield shift of the methylsulfide group to ~1.5 ppm in the ^1H NMR spectra, confirming coordination of the thioether donor atom to the ruthenium center. All new compounds were characterized

using NMR spectroscopy, thin layer chromatography, electronic absorption spectroscopy, high-resolution mass spectrometry, and elemental analysis.

4.2.2 Crystal structures

Attempts to crystallize the glycoconjugates [**1b**]$(PF_6)_2$ – [**8b**]$(PF_6)_2$ were unsuccessful and usually led to the formation of oils or colloidal suspensions. However, crystals suitable for X-ray diffraction analysis were obtained for [**5a**]Cl, and for [**3a**]PF_6 and [**4a**]PF_6 after salt metathesis of [**3a**]Cl and [**4a**]Cl using aqueous NH_4PF_6, followed by vapor diffusion of diethyl ether to a solution of [**3a**]PF_6 in acetone or acetone to a solution of [**4a**]PF_6 in ethyl acetate. Crystals suitable for X-ray diffraction for [**5a**]Cl were obtained by vapor diffusion of diisopropylether in acetonitrile. The three crystal structures showed the expected distorted octahedral geometry, with a reduced (< 180°) N-Ru-N angle for the coordinated terpyridine ligand (N1-Ru1-N3, 159.11 – 159.40°, Table 4.1). The bidentate ligands dpq, dppz and dppn are all bound perpendicular to tpy, with a N4-Ru1-N5 bite angle of 79.26 – 80.2° (Table 4.1). The Ru1-Cl1 bond lengths were found to be similar with values ranging from 2.4015 to 2.4165 Å which are very close to reported values for related complexes Selected bond lengths and angles are given in Table 4.1.[22]

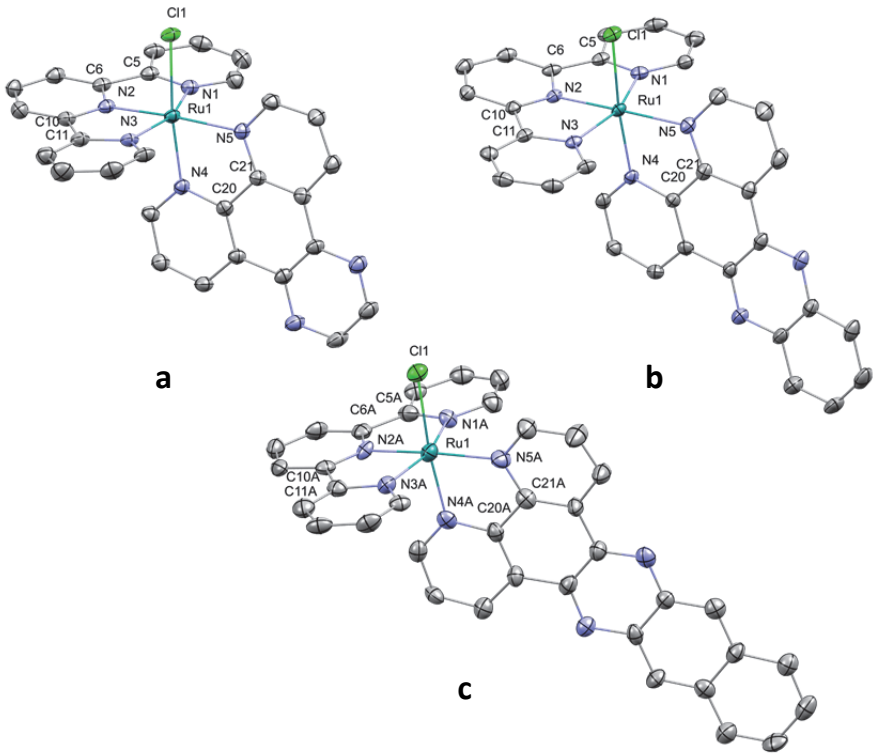

Figure 4.2. Displacement ellipsoid plots (50% probability level) of the complex cation [**3a**]PF_6, [**4a**]$PF_6.(CH_3)_2CO$ and [**5a**]Cl. For [**5a**]Cl only one of the independent molecules is shown. Hydrogen atoms, counter-ions, and lattice solvent molecules, have been omitted for clarity.

Table 4.1 Selected bond distances (Å) and bond angles (°) for complexes [**3a**]PF_6, [**4a**]$PF_6.(CH_3)_2CO$ and [**5a**]Cl.

	[**3a**]$(PF_6)_2$	[**4a**]$(PF_6)_2$	[**5a**]Cl[a]
Ru1 - Cl1	2.4062(5)	2.4015(7)	2.4165(17)
Ru1 - N1	2.069(2)	2.053(2)	2.048(5)
Ru1 - N2	1.9569(19)	1.957(2)	1.953(5)
Ru1 - N3	2.058(2)	2.064(2)	2.050(5)
Ru1 - N4	2.046(2)	2.044(2)	2.043(5)
Ru1 - N5	2.0917(19)	2.074(2)	2.073(5)
C5 - C6	1.472(3)	1.469(4)	1.469(9)
C5 - N1	1.369(3)	1.372(3)	1.389(8)
C6 - N2	1.355(3)	1.357(3)	1.340(7)
C10 - C11	1.478(3)	1.479(4)	1.484(8)
C10 - N2	1.355(3)	1.349(4)	1.340(7)
C11 - N3	1.371(3)	1.372(3)	1.384(7)
C20 - C21	1.446(3)	1.440(4)	1.459(8)
C20 - N4	1.370(3)	1.371(3)	1.370(7)
C21 - N5	1.364(3)	1.362(3)	1.379(8)
N1- Ru1 - N3	159.10(8)	159.58(9)	159.67(19)
N4 - Ru1- N5	79.45(8)	79.26(9)	80.2(2)

[a] Values for Ru1A.

4.2.3 Photophysical properties of the [Ru(tpy)(NN)(L)]$^{n+}$ complexes

The photophysical properties of the chloride complexes [**1a**]Cl – [**8a**]Cl were first investigated in acetonitrile, in which the complexes are all soluble and do not hydrolyze. The chloride complexes [**1a**]Cl – [**8a**]Cl show metal-to ligand charge transfer (^{1}MLCT) bands varying between 501 and 523 nm corresponding to the, with molar absorptivities ranging from 9.1 x 10^3 to 12.8 x 10^3 M^{-1} cm^{-1} (Table 4.2), comparable to reported values for ruthenium(II) polypyridyl complexes.[7, 11, 14b, 23] All complexes have very low phosphorescence quantum yields under deoxygenated conditions(Φ_p < 10^{-4}) except for [**2a**]Cl, [**5a**]Cl, and [**6a**]Cl that are weakly emissive (Φ_p = 10^{-3} to 10^{-4}). The $^1O_2$ generation quantum yield in CD_3OD are low ($\Phi_\Delta \leq 0.05$), with the exception of [**6a**]Cl (Φ_Δ = 8.2 x 10^{-2}), which is also the most emissive complex.

The hydrophilicity of the thioether analogues [**1b**]$(PF_6)_2$ – [**8b**]$(PF_6)_2$ allowed for studying photosubstitution quantum yields in water using electronic absorption spectroscopy. Monochromatic blue light (450 or 470 nm) was used to irradiate the complexes into their ^{1}MLCT absorption band. While all thioether complexes are thermally stable at room temperature, seven of the eight complexes, i.e., [**1b**]$(PF_6)_2$ to [**7b**]$(PF_6)_2$, showed light-induced exchange of their thioether ligand for H_2O. The ligand photosubstitution was characterized by clear isosbestic points in the UV-vis spectra (450 to 476 nm), as shown in Figure 4.3 For each of these reactions a bathochromic shift of the ^{1}MLCT band was observed, which is consistent with earlier reports on the formation of monoaqua-ruthenium complexes in aqueous solution.[14a] Most complexes have a photosubstitution quantum yield (Φ_{450}) of 0.5 – 2 percent, leading to photosubstitution reactivities ($\xi = \Phi_{450}$ x ε_{450}, where ε_{450} is the molar absorption at 450 nm) in the order of ten to hundreds (ξ = 11 – 256). Changing the bidentate ligand therefore has a significant influence on the photosubstitution rates. Interestingly, the dppz complex [**4b**]$^{2+}$ has the highest

photosubstitution quantum yield of the series, which is also ~20-fold higher (Φ_{450} = 0.020) than that of the structurally similar dppn analogue [**5b**]$^{2+}$, which showed the lowest Φ_{450} (0.00095).[13b] Furthermore, [**4b**]$^{2+}$ produced minimal amounts of $^1O_2$ (Φ_Δ = 0.0010) and is poorly emissive (Φ_P = < 1 x 10^{-5}), which indicated that contrary to the dppn complex [**5b**]$^{2+}$ for which light irradiation leads to low-lying $^3\pi\pi^*$ excited states located on the spectator bidentate ligand.[13b] With the dppz complex such $^3\pi\pi^*$ states are either too high in energy to be populated, or outcompeted by a rather quick conversion to the photodissociative metal-centered triplet state (^{3}MC).

Another interesting observation concerned the difference in reactivity between [**7b**]$^{2+}$ and [**8b**]$^{2+}$. Whereas [**7b**]$^{2+}$ displayed ligand dissociation efficiency comparable to that of the bpy complex [**1b**]$^{2+}$, the azpy compound [**8b**]$^{2+}$ did not show any ligand photosubstitution, indicating a strong electronic effect of the azo ligand on the photoreactivity of its ruthenium complex. The ^{1}MLCT absorption maximum for [**8b**]$^{2+}$ is significantly lower in energy (505 nm) than that of [**7b**]$^{2+}$ (472 nm), which points to the low energy of the azo-based π^* orbital of the azpy ligand, leading to a low-lying ^{3}MLCT state for the complex. Since there is no steric strain in this complex to lower the ^{3}MC state,[23b] the ^{3}MC–^{3}MLCT energy gap is very large in [**8b**]$^{2+}$, therefore preventing photosubstitution reactions to occur. It should be noted that [**8b**]$^{2+}$ is not emissive at all (Φ_P < 1 x 10^{-5}) and has a negligible $^1O_2$ generation quantum yield (0.007), and thus that non-radiative decay is the main deactivation pathway for this complex. Regarding $^1O_2$ generation, most of the other complexes produced small amounts of $^1O_2$ in CD_3OD (Φ_Δ = 0.002 – 0.14), with the exception of [**5b**]$^{2+}$ with a $^1O_2$ quantum yield of 0.71.[13b] Interestingly, its chloride analogue [**5a**]$^+$ only has a $^1O_2$ quantum yield of 0.023 under the same conditions, emphasizing the critical influence of the monodentate ligand on the photochemical and photosensitizing properties of this family of complexes.

Table 4.2 Lowest-energy absorption maxima (λ_{max}), molar absorption coefficients at λ_{max} (ε_{max} in $M^{-1}cm^{-1}$) and λ_{450} (ε_{450} in $M^{-1}cm^{-1}$), photosubstitution quantum yields (Φ_{450}) at 298 K, $^1O_2$ quantum yields (Φ_Δ) at 293 K, photosubstitution reactivity (ξ = $\Phi_{450} \times \varepsilon_{450}$), and phosphorescence quantum yield (Φ_P) at 293 K for complexes [**1a**]Cl-[**8a**]C and, [**1b**]$(PF_6)_2$ - [**8b**]$(PF_6)_2$.

Complex	λ_{max} in nm (ε_{max} in $M^{-1}cm^{-1}$)[a]	ε_{450} ($M^{-1}cm^{-1}$)	Φ_{450}[b]	ξ	Φ_Δ[c]	Φ_P[c]
[**1a**]Cl	504 (9.1 x 10^3)	4.6 x 10^3	-	-	0.055	< 1 x 10^{-5}
[**2a**]Cl	501 (9.1 x 10^3)	6.5 x 10^3	-	-	0.048	8.5 x 10^{-4}
[**3a**]Cl	504 (9.1 x 10^3)	6.6 x 10^3	-	-	0.055	< 1 x 10^{-5}
[**4a**]Cl	511 (9.6 x 10^3)	5.6 x 10^3	-	-	0.005	< 1 x 10^{-5}
[**5a**]Cl	498 (12.0 x 10^3)	8.5 x 10^3	-	-	0.023	4.3 x 10^{-4}
[**6a**]Cl	501 (1.12 x 10^3)	6.8 x 10^3	-	-	0.082	3.2 x 10^{-3}
[**7a**]Cl	523 (13.0 x 10^3)	3.4 x 10^3	-	-	0.012	1.4 x 10^{-5}
[**8a**]Cl	508 (12.2 x 10^3)	3.9 x 10^3	-	-	< 0.001	1.8 x 10^{-5}
[**1b**]$(PF_6)_2$	450 (7.0 x 10^3)	7.0 x 10^3	0.0084	59	0.020 (0.020)	< 1 x 10^{-5}
[**2b**]$(PF_6)_2$	448 (6.2 x 10^3)	6.2 x 10^3	0.0065	40	0.050 (0.080)	1.2 x 10^{-4}
[**3b**]$(PF_6)_2$	448 (8.9 x 10^3)	8.9 x 10^3	0.0067	60	0.030 (0.010)	< 1 x 10^{-5}
[**4b**]$(PF_6)_2$	458 (13.1 x 10^3)	12.8 x 10^3	0.020	256	0.0010 (0.0030)	< 1 x 10^{-5}
[**5b**]$(PF_6)_2$	458 (11.6 x 10^3)	11.4 x 10^3	0.00095	11	0.71/(0.41)	< 1 x 10^{-5}
[**6b**]$(PF_6)_2$	460 (11.0 x 10^3)	10.4 x 10^3	0.0070	73	0.0020	< 1 x 10^{-5}
[**7b**]$(PF_6)_2$	472 (11.7 x 10^3)	11.7 x 10^3	0.0053	62	0. 11 (0.14)	2.5 x 10^{-3}
[**8b**]$(PF_6)_2$	505 (7.2 x 10^3)	2.7 x 10^3	-	-	0.0070(-)	< 1 x 10^{-5}

[a]. In MeCN for [**1a**]Cl – [**8a**]Cl and in MilliQ H_2O for [**1b**]$(PF_6)_2$ – [**8b**]$(PF_6)_2$. [b] in H_2O. λ_{irr} = 450 nm for [**1b**]$(PF_6)_2$ – [**6b**]$(PF_6)_2$ and 470 nm for [**7b**]$(PF_6)_2$. [c] in CD_3OD.

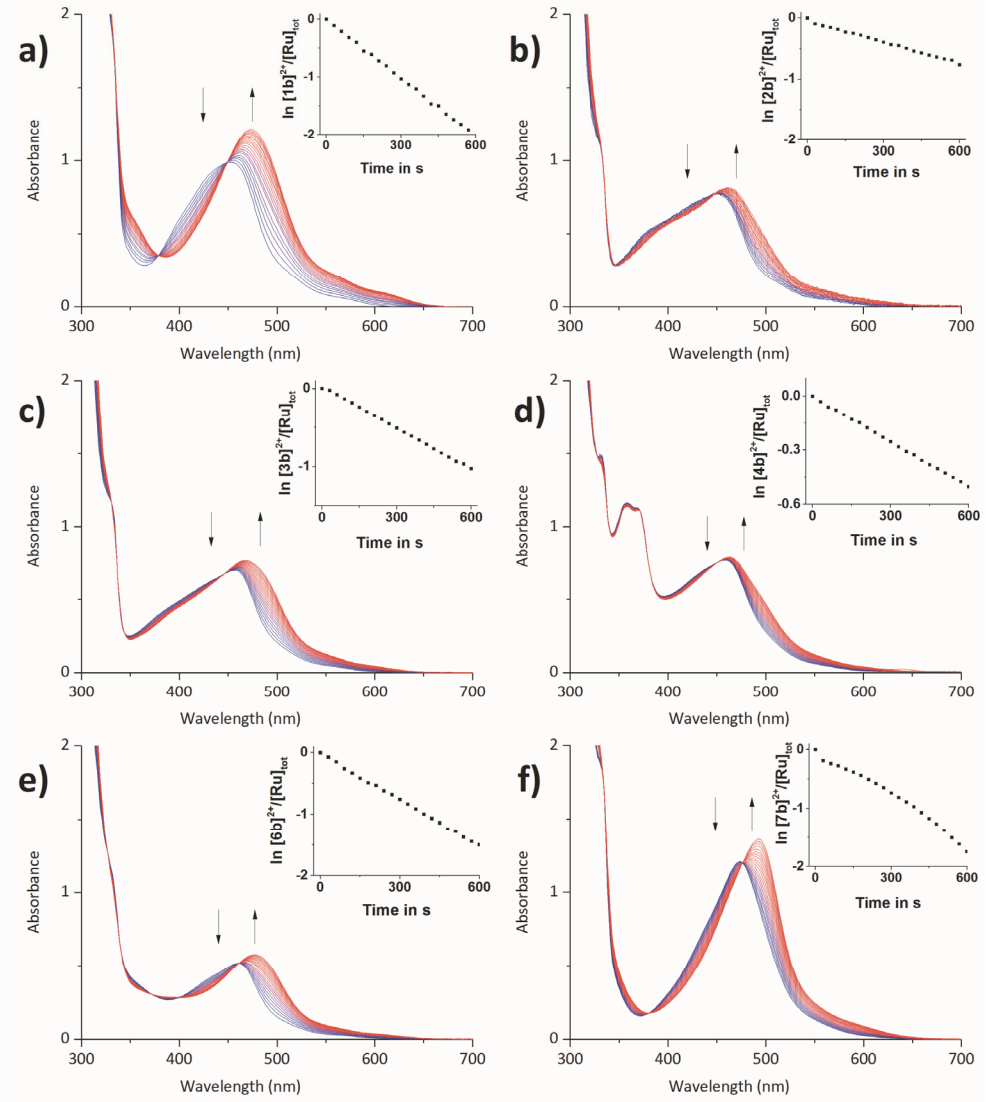

Figure 4.3. Electronic absorption spectra of [**1b**]$(PF_6)_2$ - [**4b**]$(PF_6)_2$, [**6b**]$(PF_6)_2$ and [**7b**]$(PF_6)_2$ in deoxygenated H_2O upon irradiation at 450 or 470 nm for 5 min at T = 298 K. Spectra measured every 30 s. a) [**1b**]$(PF_6)_2$, $[Ru]_{tot} = 1.38 \times 10^{-4}$ M, λ_{exc} = 450 nm, photon flux = 1.71×10^{-7} mol s^{-1}. b) [**2b**]$(PF_6)_2$, $[Ru]_{tot} = 1.15 \times 10^{-4}$ M, λ_{exc} = 450 nm, photon flux = 6.83×10^{-8} mol s^{-1}. c) [**3b**]$(PF_6)_2$, $[Ru]_{tot} = 7.91 \times 10^{-5}$ M, λ_{exc} = 450 nm, photon flux = 5.29×10^{-8} mol s^{-1}. d) [**4b**]$(PF_6)_2$, $[Ru]_{tot} = 8.66 \times 10^{-5}$ M, λ_{exc} = 450 nm, photon flux = 2.84×10^{-8} mol s^{-1}. e) [**6b**]$(PF_6)_2$, $[Ru]_{tot} = 4.75 \times 10^{-5}$ M, λ_{exc} = 450 nm, photon flux = 4.97×10^{-8} mol s^{-1}. f) [**7b**]$(PF_6)_2$, $[Ru]_{tot} = 8.88 \times 10^{-5}$ M, λ_{exc} = 470 nm, photon flux = 1.52×10^{-7} mol s^{-1}. Inset depicts the evolution of Ln $[Ru]_{SRR'}/[Ru]_{tot}$ vs. irradiation time in s, where $[Ru]_{SRR'}$ represents the concentration of ruthenium-thioether complex at time t, and $[Ru]_{tot}$ the total ruthenium concentration.

4.2.4 Cytotoxicity

The cytotoxic properties of the chloride complexes [**1a**]Cl - [**8a**]Cl and their caged analogues [**1b**]$(PF_6)_2$ - [**8b**]$(PF_6)_2$ were evaluated against two different human cell lines: A549 (human lung carcinoma) and MCF-7 (human breast adenocarcinoma). Considering the photo-substitution properties of some of these complexes, their photocytotoxicity was also tested under blue light irradiation (3.2 ± 0.2 J·cm^{-2} at 454 ± 11 nm) as described previously for [**5b**]$(PF_6)_2$.[13b] Cells were seeded at t = 0, treated after 24 h with a concentration gradient of each ruthenium complex, irradiated or maintained in the dark after replacing the media, and further incubated in the dark for 48 h. At t = 96 h cell viability was determined using the sulforhodamine B (SRB) assay.[24] The effective concentrations (EC_{50}), defined as the concentration at which a 50% survival rate on cell viability is observed, are reported in Table 4.3. Most chloride complexes were found to be non-cytotoxic, with the exception of [**8a**]Cl that was found moderately cytotoxic (EC_{50} = 28 µM) against the MCF-7 cell line, in agreement with the value reported by Reedijk et al.[25] The values for [**4a**]Cl (59 µM and 34 µM against A549 and MCF-7, respectively) were found similar to that observed for $[Ru(bpy)(dppz)_2]^{2+}$ analogues reported by the group of Schatzschneider.[26] Based on their results, it was expected that the structurally similar but more lipophilic dppn complex [**5a**]Cl would be cytotoxic, but no significant toxicity was observed for this complex. On the other hand, its EC_{50} could not be clearly determined due to the poor solubility of this complex in cell culture medium.[13b] Interestingly however, [**5a**]Cl was found to be cytotoxic upon blue light irradiation, with EC_{50} values of 9.7 µM and 3.2 µM for A549 and MCF-7 cells, respectively, corresponding to photoindexes (PI) of more than 2.6 and 7.9, respectively. This result is unexpected, since the $^1O_2$ quantum yield of [**5a**]Cl (0.023) is much lower than that of its glycoconjugated analogue [**5b**]$(PF_6)_2$ (0.71). A possible explanation would be the partial conversion, after uptake, of the chloride complex to its aquated counterpart $[Ru(tpy)(dppn)(H_2O)]^{2+}$ (Figure 4.4a), which has been demonstrated to be a good $^1O_2$ sensitizer as demonstrated by close analogue $[Ru(tpy)(dppn)(CD_3OD)]^{2+}$ (Φ_Δ = 0.43).[13b] An alternative explanation, would be that a different type of PDT is occurring, such as PDT type I, which is dependent upon the formation of radical species without intervention of molecular oxygen.[27] Further studies would be needed to conclude on the biological mechanism of the photocytoxicity of [**5a**]Cl.

None of the glycoconjugated complexes were found photocytotoxic except [**5b**]$(PF_6)_2$, which was recently reported to enter passively into the cells and to destroy mitochondrial DNA by singlet oxygen generation.[13b] In our standard treatment protocol, media is replaced before light irradiation. In such conditions, photocytotoxicity can solely rely on the molecules that have been taken up by the cells during incubation, which may be a problem for highly hydrophilic glucose-conjugates such as [**1b**]$(PF_6)_2$ – [**8b**]$(PF_6)_2$ (see below). For compound [**4b**]$(PF_6)_2$, an adjustment of the protocol, consisting in irradiating the cells without media refreshing, led to a modest but clearly improved PI (2.4 and 2.6 for

MCF-7 and A549, respectively). With such a protocol the full dose of compound added to each well remains present during and after irradiation, and most importantly activation may occur outside the cell, and be followed by cellular uptake of the activated photoproduct. For [**4b**]$(PF_6)_2$, the observed phototoxicity might thus be explained by the formation of the aquated species $[Ru(tpy)(dppz)(H_2O)]^{2+}$ outside the cell, followed by *in situ* conversion to the chloride species [**4a**]Cl due to the high chloride content in media (>100 mM), followed by cellular uptake (Figure 4.4b). This interpretation is supported by the EC_{50} values found for [**4a**]Cl, which were not impressive but could clearly be measured (59 µM and 34 µM for A549 and MCF-7 respectively). Not refreshing the media before light activation did not lead to enhanced toxicity for [**1b**]$(PF_6)_2$ – [**3b**]$(PF_6)_2$ and for [**6b**]$(PF_6)_2$ – [**7b**]$(PF_6)_2$, showing that keeping high concentrations of the prodrug during and after light irradiation does not necessarily lead to enhanced phototoxicity. Overall, these results demonstrate that [**4b**]$(PF_6)_2$ is a moderately effective PACT agent,[3b] whereas the dppn analogues [**5a**]Cl and [**5b**]$(PF_6)_2$ are catalytic PDT sensitizers which can be activated using a low dose of blue light. They also demonstrate that apparently minor differences in the treatment protocol of light-activated drugs may lead to very different interpretation of the cytotoxicity of light-activated compounds.

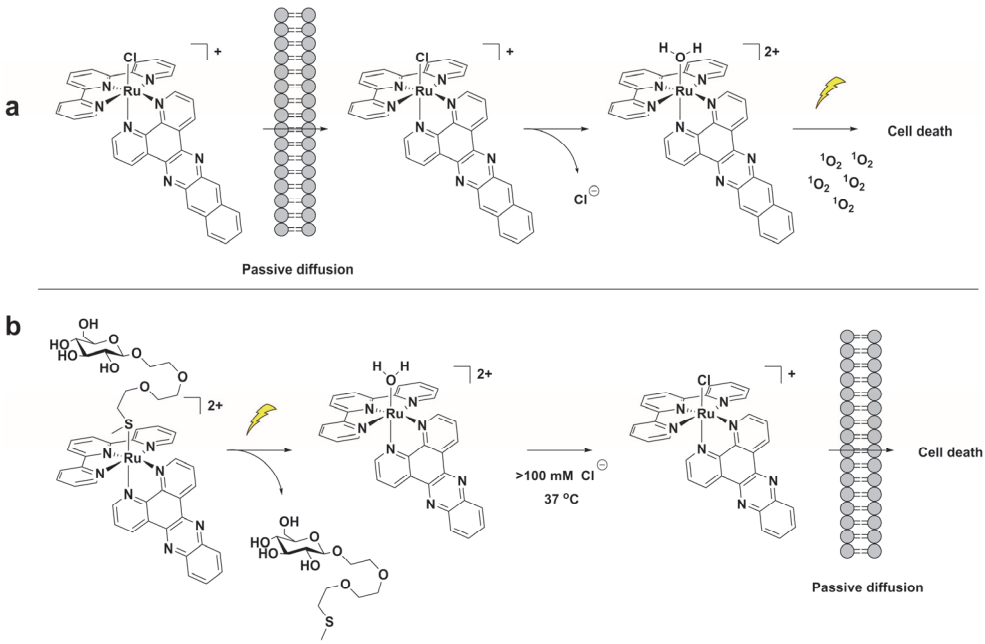

Figure 4.4. Proposed mechanisms for light-induced toxicity for a) [**5a**]Cl with media replacement, and b) [**4b**]$(PF_6)_2$ without media replacement. The lipid bilayer represents the cell membrane.

Table 4.3 Cytotoxicity of compounds [**1a**]Cl – [**8a**]Cl and [**1b**]$(PF_6)_2$ – [**8b**]$(PF_6)_2$ towards A549 and MCF-7 cells in the dark and upon blue light irradiation (454 nm, 3.2 J.cm^{-2}). Cell-growing inhibition effective concentrations (EC_{50}) are reported in μM with 95% confidence interval (CI) in μM. Data is the mean over three independent experiments. Photocytotoxicity index (PI) = $EC_{50dark}/EC_{50light}$.

Complex[a]	Light Dose (J cm^{-2})	A549 EC_{50}	CI	PI	MCF-7 EC_{50}	CI	PI
[**1a**]Cl	0	>100			>100		
	3.2	>100		-	>100		-
[**2a**]Cl	0	>100			64	+12	
				-		-9.1	
	3.2	>100			52	+15	1.2
						-10	
[**3a**]Cl	0	>100			>100		-
	3.2	>100		-	>100		
[**4a**]Cl	0	59	+31		34	+6.0	
			-21	1.3		-5.1	1.1
	3.2	47	+19		31	+4.8	
			-13			-4.2	
[**5a**]Cl	0	>25			>25		
	3.2	9.7	+4.4	>2.6	3.2	+1.3	>7.9
			-2.6			-0.87	
[**6a**]Cl	0	>25			>25		
	3.2	>25		-	>25		-
[**7a**]Cl	0	>100			>100		
	3.2	>100		-	>100		-
[**8a**]Cl	0	>100			28	+4.9	
				-		-4.2	-
	3.2	-			-		
[**1b**]$(PF6)_2$	0	>100			>100		
	3.2	>100		-	>100		-
[**2b**]$(PF6)_2$	0	>100			>100		
	3.2	>100		-	>100		-
[**3b**]$(PF6)_2$	0	>100			>100		
	3.2	>100		-	>100		-
[**4b**]$(PF6)_2$	0	>100			>100		
	3.2	>100		-	>100		-
[**4b**]$(PF6)_2$[b]	0	64	+17		52	+12	
			-13	2.4		-9.4	2.6
	3.2	27	+6.4		20	+2.5	
			-5.2			-2.2	
[**5b**]$(PF6)_2$[c]	0	19	+4.0		9.6	+2.9	
			-3.3	26		-2.3	11
	3.2	0.72	+0.16		0.86	+0.21	
			-0.13			-0.17	
[**6b**]$(PF6)_2$	0	>100			>100		
	3.2	>100		-	>100		-
[**7b**]$(PF6)_2$	0	>100		-	>100		-
	3.2	>100			>100		
[**8b**]$(PF6)_2$	0	>100		-	>100		-
	3.2	>100			>100		

[a] Normal protocol: Cells were incubated with compound for 24 h, followed by replacement of the media, kept in the dark, or irradiated with blue light (5 min at 454 nm , 10.5 mW·cm^{-2}, 3.2 J.cm^{-2}). [b] As in normal protocol, without replacing media during treatment (cells are irradiated in the presence of compound). [c] Ref [13b].

4.2.5 Log $P_{o/w}$ and uptake

To acquire more insight on the effect of glycoconjugation on the solubility, cellular uptake, and toxicity of these complexes, the water-octanol partition coefficients (log $P_{o/w}$) were determined for all complexes according to reported standards (Figure 4.5b).[28] As shown in Figure 4.5b (left) the chloride compounds with the smallest bidentate ligands, i.e., [**1a**]Cl – [**3a**]Cl, have similar log $P_{o/w}$ values ranging from -0.81 to -1.1, while [**7a**]Cl and [**8a**]Cl

have log $P_{o/w}$ values of -1.60 to -1.80. For these five complexes the chloride counter anion provides appreciable water solubility. By contrast, the chloride compounds with the largest bidentate ligands, i.e., [**4a**]Cl – [**6a**]Cl, are much more hydrophobic with log $P_{o/w}$ values ranging from -0.10 to +1.0. Whereas one may expect that the dicationic nature of [**1b**]$(PF_6)_2$ – [**8b**]$(PF_6)_2$ and glycoconjugation should improve water solubility compared to their chloride analogues, we found that [**1b**]$(PF_6)_2$ – [**3b**]$(PF_6)_2$ had similar log $P_{o/w}$ values (-0.11 to -0.51, respectively) compared to their analogues [**1a**]Cl – [**3a**]Cl, while [**7b**]$(PF_6)_2$ and [**8b**]$(PF_6)_2$ were slightly more hydrophobic (log $P_{o/w}$ = -0.20 and -0.18, respectively) than [**7a**]Cl and [**8a**]Cl. This result points to the critical influence of the counterions, as the two hexafluoridophosphate anions of the glycoconjugate compounds increase lipophilicity, compared to chlorides. Furthermore, the chloride complexes are not stable in water, resulting in (partial) conversion to the [Ru(tpy)(N-N)(H_2O)]Cl_2 species which are more soluble in water than the hexafluoridophosphate salts of the R-substituted ruthenium complexes. The most hydrophobic chloride complexes [**4a**]Cl – [**6a**]Cl, that were much more difficult to dissolve in water, profited most of glycoconjugation, as [**4b**]$(PF_6)_2$ – [**6b**]$(PF_6)_2$ indeed became water soluble (log $P_{o/w}$ = -0.84 to -0.50, respectively). Overall glycoconjugation allowed for investigating the photochemistry of *all* thioether complexes [**1b**]$(PF_6)_2$ – [**8b**]$(PF_6)_2$ in water.

In order to check whether the low toxicity of the thioether-glucose conjugates was not simply due to a low uptake, cellular uptake was studied for all sixteen complexes in A549 cells at a concentration of 25 µM, using an incubation time of 24 h and measuring intracellular ruthenium concentrations by ICP-MS. Although no general correlation could be found between the log $P_{o/w}$ values for these complexes and their cellular uptake, very strong differences in metal uptake were observed depending on the ligands and counterions (Figure 4.5a). The most hydrophobic chloride compounds [**4a**]Cl, [**5a**]Cl and [**6a**]Cl displayed very high metal uptake (>1000 ng Ru per million cells), while their glycoconjugates [**4b**]$(PF_6)_2$, [**5b**]$(PF_6)_2$ and [**6b**]$(PF_6)_2$ displayed cellular uptake that was much lower (10 - 20 ng Ru per million cells, e.g. 250 times lower for [**5b**]$(PF_6)_2$ compared to [**5a**]Cl). Of course, this lower uptake can partially be explained by the lower log $P_{o/w}$ values of the glycoconjugates, and at least for [**5b**]$(PF_6)_2$, by the absence of GLUT-based active uptake.[13b] However, [**4b**]$(PF_6)_2$ – [**6b**]$(PF_6)_2$ are also taken up in 10-fold higher amounts than [**1b**]$(PF_6)_2$ – [**3b**]$(PF_6)_2$, which have comparable log $P_{o/w}$ values. These results may not necessarily represent the conditions experienced by these compounds at the cell membrane, for which it is more likely that the lipophilic PF_6^- counterions are already exchanged for the more abundant and more water soluble chloride or phosphate anions in the buffer, canceling the effect of the PF_6 anion on lipophilicity.

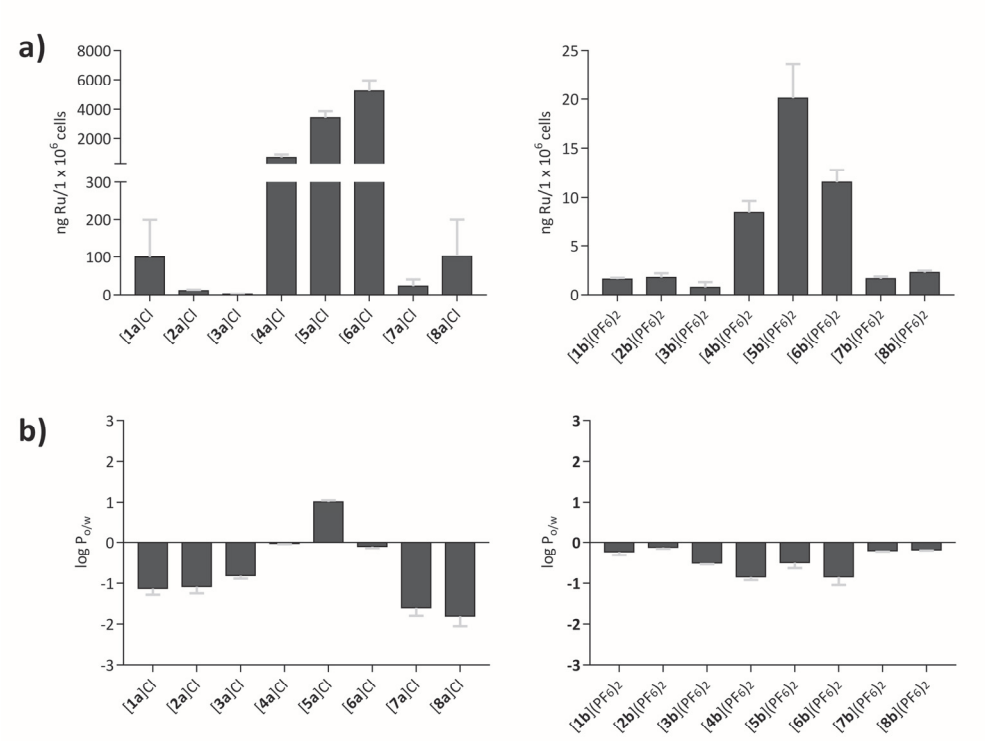

Figure 4.5. a). Intracellular uptake of 25 μM of [**1a**]$(PF_6)_2$– [**8a**] (left) and [**1b**] – [**8b**]$(PF_6)_2$ (right) in A549 cells after 24 h. Values are reported ± SD, n = 2. **b).** Log $P_{o/w}$ values found for [**1a**]Cl – [**8a**]Cl (left) and [**1b**]$(PF_6)_2$ – [**8b**]$(PF_6)_2$ (right). Values are reported ± SD, n = 3.

4.3 Discussion

Some of the chloride complexes [**1a**]Cl – [**8a**]Cl were thermally unstable in water and therefore no photodissociation quantum yields were determined, while their singlet oxygen properties were in general very low. The phototoxicity in the series of the most lipophilic compounds [**4a**]Cl-[**6a**]Cl cannot be explained by the trends observed in cell uptake and singlet oxygen generation. [**6a**]Cl has a higher singlet oxygen quantum yield (0.082) than [**4a**]Cl and [**5a**]Cl (0.005 and 0.023, respectively), but it is not phototoxic whereas [**4a**]Cl and [**5a**]Cl are. At the same time all three complexes are taken up in high amounts. In this series of complexes different intracellular localization or biological targets, coupled to unknown photoreactions of [**5a**]Cl, must explain the differences in phototoxicity between [**6a**]Cl on the one hand and [**4a**]Cl and [**5a**]Cl on the other hand.

An opposite conclusion can be drawn for the glycoconjugates series [**4b**]$(PF_6)_2$, [**5b**]$(PF_6)_2$ and [**6b**]$(PF_6)_2$. The only phototoxic agent of this series, [**5b**]$(PF_6)_2$, has by far the highest singlet oxygen quantum yield (0.71 vs. 0.0010 and 0.0020), while all three compounds are taken up in similar amounts (10-20 ng Ru per million cells). Hence, [**5b**]$(PF_6)_2$ is an excellent PDT agent, while a PACT mode of action cannot be ruled out considering the

phototoxic properties of [**5a**]Cl and its low singlet oxygen quantum yield. The phototoxicity observed for [**4b**]$(PF_6)_2$ when the medium is not refreshed before irradiation, suggests that this compound may act as a cytotoxic PACT agent. Furthermore, [**4b**]$(PF_6)_2$ showed the highest photosubstitution quantum yield (0.02) and no significant singlet oxygen production. When cell-culture media was replaced before light irradiation, the glycoconjugate compound was not taken up in high amounts, and given the poor photodynamic properties of the photoproduct ([**4a**]$^+$ or $[Ru(tpy)(dppz)(OH_2)]^{2+}$) not enough reactive oxygen species could be generated to kill the cells. This example demonstrates that the potential of [**4b**]$(PF_6)_2$ as a PACT agent is determined by the treatment protocol, which should be taken into account in further PACT studies. Furthermore, this complex has been shown to act has a DNA light-switch in the presence of DNA, which might be useful for theranostic applications.[29]

4.4 Conclusion

Overall, eight chloride terpyridine complexes [**1a**]Cl – [**8a**]Cl with eight different bidendate spectator chelating ligands, and their eight thioether-glucose conjugates, were synthesized, to compare the corresponding photophysical properties, photoreactivity, water solubility, cellular uptake, and phototoxicity. Depending on the bidentate ligand these complexes can be considered either for photocaging, or for PACT and/or PDT. Compound [**8a**]Cl is not suitable for photocaging or phototherapy because the azo group of the azpy spectator ligand stabilizes the ^{3}MLCT state too much and prevents thermal population of the ^{3}MC state, thereby quenching photosubstitution. Singlet oxygen generation was also fully quenched in [**8a**]Cl and [**8b**]$(PF_6)_2$, emphasizing the poor photosensitizing properties of this compound. The five complexes [**1a**]Cl − [**3a**]Cl, [**6a**]Cl, and [**7a**]Cl, are non-toxic, and once substituted by thioethers they form complexes with similar photosubstitution quantum yields (Φ_{450} ~ 0.01) and low $^1O_2$ production quantum yields (Φ_Δ < 0.10). As a consequence, they are excellent candidates for the photocaging of thioether-based biologically active compounds such as the antibiotics amoxicillin and clindamycin. The exceptionally high cellular uptake measured for [**6a**]Cl is worth noticing (5220 ± 737 ng Ru per million cells), considering that this compound did not show any measurable cytotoxicity at concentrations lower than 25 µM. It can even turn highly hydrophilic compounds such as R into species such as [**6b**]$(PF_6)_2$ that are still lipophilic enough to enter into cancer cells. Finally, [**4a**]Cl and [**5a**]Cl show similar lipophilicity compared to [**6a**]Cl and comparably high cellular uptake, but they also showed some toxicity both in the dark and after light activation. They are therefore less interesting as PACT carriers and instead have better potential as a either a cytotoxic PACT agent or for PDT as we have recently demonstrated for [**5b**]$(PF_6)_2$.[13b] Overall, this work demonstrates that complexes based upon the $[Ru(tpy)(N\text{-}N)(L)]^{n+}$ scaffold are good photocaging agents

but poorly (photo)cytotoxic unless DNA intercalators such as dppz and dppn are chosen as a bidentate ligand, in which case they could serve as phototoxic agents.

4.5 Experimental

4.5.1 General

Reagents were purchased from Sigma-Aldrich and used without further purification. Dpq,[30] dppz,[30] dppn,[31] pmip,[32] azpy[33] and pymi[34] were synthesized according to reported procedures. 2-(2-(2-(methylthio)ethoxy)ethoxy)ethyl-β-D-glucopyranoside and [**1b**]$(PF_6)_2$ were synthesized as described in Chapter 2. [Ru(tpy)Cl_3],[35] [Ru(tpy)(bpy)Cl]Cl,[16] [Ru(tpy)(phen)Cl]Cl,[17] [Ru(tpy)(azpy)Cl]Cl,[20] [Ru(tpy)(pymi)Cl]Cl,[19] [Ru(tpy)(dppz)Cl]Cl,[18] and [Ru(tpy)(dppn)Cl]Cl,[13b] were synthesized according to known literature procedures. 2,2′:6′,2′′-Terpyridine (tpy) was obtained from ABCR GmbH & Co. Dry solvents were collected from a Pure Solve MD5 solvent dispenser from Demaco Holland BV. Solvents were deoxygenated by bubbling argon through the solution for 30 minutes and all inorganic reactions and were carried out under an inert atmosphere in the dark, unless stated otherwise. Solvents were removed under vacuum with a rotary evaporator in the dark at 30 °C, unless stated otherwise. Flash chromatography was performed on silica gel (Screening devices B.V.) with a particle size of 40 - 64 μM and a pore size of 60 Å. TLC analysis was conducted on TLC aluminium foils with silica gel matrix (Supelco, silica gel 60, 56524) with detection by UV-absorption (254 nm), by spraying with 10% H_2SO_4 in ethanol or with a solution of $NH_4Mo_7O_{24}.4H_2O$ 25 g/L, $NH_4CeSO_4.H_2O$ 10 g/L, 10% H_2SO_4 in H_2O, followed by charring at ~250 °C on a heating plate. NMR spectra were recorded on a Bruker AV-400, AV-500 or AV-850. ^{1}H NMR and ^{13}C NMR were recorded in CD_3OD and $(CD_3)_2CO$ with chemical shift (δ) relative to the solvent peak. High resolution mass spectra were recorded by direct injection (2 μl of 2 μM solution in water/acetonitrile; 50/50; v/v and 0.1% formic acid) in a mass spectrometer (Thermo Finnigan LTQ Orbitrap) equipped with an electrospray 250 °C) with resolution R = 60000 at m/z 400 (mass range m/z = 150 – 2000) and dioctylphtalate (m/z = 391.28428) as a lock mass. The high-resolution mass spectrometer was calibrated prior to measurements with a calibration mixture (Thermo Finnigan).

4.5.2 Synthesis

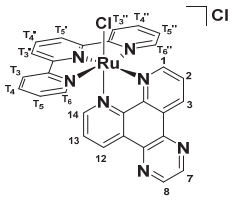

[Ru(tpy)(dpq)Cl]Cl, [3a]Cl: [Ru(tpy)Cl_3] (103 mg, 0.234 mmol) and dpq (54.0 mg, 0.233 mmol) were dissolved in deoxygenated EtOH/H_2O (4 mL, 4:1), Et_3N (35 uL, 0.25 mmol) was added and the mixture was heated at reflux for 4 h. The mixture was filtered over Celite®, the volume reduced by ~50% and the filtrate was allowed to cool overnight at 4 °C. The resulting precipitate was collected on a glas frit, washed with water (3 x 50 mL), and 1M HCl (3 x 50 mL), which, after drying

under high vacuum, afforded the title compound as a purple solid. (146 mg, 0.229, 98%). R_f = 0.61 (10% MeOH in DCM); ^{1}H NMR (400 MHz, CD_3OD) δ = 10.53 (d, *J* = 5.4 Hz, 1H, 1), 9.85 (d, *J* = 8.3 Hz, 1H, 3), 9.27 (m, 2H, 8, 12), 9.19 (d, *J* = 2.6 Hz, 1H, 7), 8.72 (d, *J* = 8.2 Hz, 2H, T_3', T_5'), 8.56 (d, *J* = 8.0 Hz, 2H, T_6, T_6''), 8.51 (dd, *J* = 8.5, 5.1 Hz, 1H, 2), 8.23 (t, *J* = 8.1 Hz, 1H, T_4'), 7.95 – 7.84 (m, 3H, T_5'', T_5, 14), 7.67 (d, *J* = 5.5 Hz, 2H, T_3, T_3''), 7.54 (dd, *J* = 8.5, 5.1 Hz, 1H, 13), 7.27 – 7.17 (m, 2H, T_4'',T_4).^{13}C NMR (101 MHz, CD_3OD) δ = 160.2 (C_q Arom), 159.7 (C_q Arom), 155.4 (C_H 1), 154.9 (C_H 14), 153.7 (C_H T_3, T_3''), 152.2 (C_q Arom), 150.3 (C_q Arom), 147.8 (C_H 8), 147.6 (C_H 7), 141.5 (C_q Arom), 141.1 (C_q Arom), 138.5 (C_H T_5'', T4), 135.8 (C_H T_4'), 133.6 (C_H 3), 132.4 (C_H 12), 131.2 (C_q Arom), 130.9 (C_q Arom), 128.5 (C_H 2), 127.9 (C_H T_4' T_4), 127.1 (C_H 13), 124.9 (C_H T_6'', T_6), 123.8 (C_H T_3', T_5'). HRMS: m/z calcd for $[C_{29}H_{19}N_7RuCl_2 - Cl]^+$: 602.04285, found: 602.04531; Elemental analysis calcd (%) for **[3b](PF$_6$)$_2$**.4H_2O: C, 49.09; H, 3.84; N, 13.82; found: C, 50.58; H, 3.96; N, 13.86.

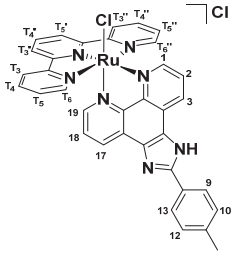

[Ru(tpy)(pmip)Cl]Cl, [6a]Cl: A mixture of [Ru(tpy)Cl_3] (0.252 g, 0.571 mmol), the ligand pmip (0.276 g, 0.888 mmol), and LiCl (0.216 g, 5.10 mmol) in EtOH/H_2O (3:1, 40 mL), was refluxed for 5 minutes under an inert atmosphere, after which Et_3N (80.0 µL, 0.571 mmol) was added. The reaction was allowed to stir for an additional 10 minutes at reflux after which it was filtered hot over Celite®. The volume of the filtrate was then reduced by ~ 50% and cooled at 4 °C overnight, which allowed the formation of a precipitate which was collected by filtration. After washing with H_2O (4 x 30 mL) the crude precipitate was further purified using a silica column (20% MeOH in DCM), which afforded [**6a**]Cl as a brown powder. (211 mg, 0.295 mmol, 52%). R_f = 0.64 (10% MeOH in DCM); ^{1}H NMR (850 MHz, CD_3OD) δ = 10.39 (d, *J* = 5.1 Hz, 1H, 1), 9.33 (d, *J* = 8.3 Hz, 1H, 3), 8.75 (d, *J* = 8.0 Hz, 1H, 19), 8.70 (d, *J* = 8.2 Hz, 2H, T_3', T_5'), 8.54 (d, *J* = 8.1 Hz, 2H, T_6'', T_6), 8.40 (dd, *J* = 8.3, 5.0 Hz, 1H, 2), 8.20 (dd, *J* = 21.9, 8.1 Hz, 3H, T_4', 9, 13), 7.89 (t, *J* = 7.7 Hz, 2H, T_5'', T_5), 7.64 (d, *J* = 5.4 Hz, 1H, 17), 7.60 (d, *J* = 5.6 Hz, 2H, T_3'', T_3), 7.45 (d, *J* = 8.1 Hz, 2H, 10, 12), 7.41 (dd, *J* = 8.1, 5.4 Hz, 1H, 18), 7.20 (t, *J* = 6.6 Hz, 2H, T_4, T_4''), 2.47 (s, 3H, CH_3). ^{13}C NMR (214 MHz, CD_3OD) δ = 160.3 (C_q Arom), 159.8 (C_q Arom), 153.5 (C_H T_3'', T_3), 152.0 (C_H 1), 151.0 (C_H 17), 148.6 (C_q Arom), 146.7 (C_q Arom), 142.1 (C_q Arom), 138.3 (C_H T_5'', T_5), 135.5 (C_H T_4), 130.9 (C_H 10, 12), 130.6 (C_H 3), 129.5 (C_H 19), 128.5 (C_H T_4, T_4''), 128.0 (C_H 9, 13), 126.7 (C_H 2), 125.9 (C_H 18), 124.8 (C_H T_6'', T_6), 123.7 (C_H T_5', T_3'), 21.5 (CH_3). HRMS: m/z calcd for $[C_{35}H_{25}N_7RuCl_2 - Cl]^+$: 680.08980, found: 680.09151; Elemental analysis calcd (%) for [**6a**]Cl.2.5H_2O: C, 55.27; H, 3.98; N, 12.89; found: C, 55.57; H, 3.97; N, 12.57.

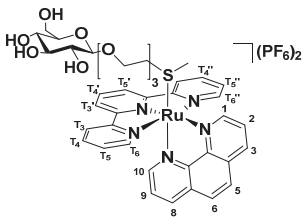

[Ru(tpy)(phen)(R)](PF$_6$)$_2$, [2b](PF$_6$)$_2$: A mixture of [Ru(tpy)(phen)Cl] (54.0 mg, 0.0992 mmol) and 2-(2-(2-(methylthio)ethoxy)ethoxy)ethyl-β-D-glucopyranoside (94.0 mg, 0.275 mmol) in deoxygenated H_2O (15 mL) was allowed

to stir at 80 °C for 16 h, after which ~200 mg NH_4PF_6 was added. Concentration *in vacuo* was followed by purification of the crude over a Sephadex LH-20 column (MeOH), by collection of the orange fraction. Removal of the solvents under vacuum afforded [**2b**]$(PF_6)_2$ as a red solid. (80.3 mg, 0.0767, 83%). R_f = 0.64 (acetone/water/sat. KPF_6 100/80/20); ^{1}H NMR (400 MHz, CD_3OD) δ = 10.17 (d, *J* = 5.1 Hz, 1H, 1), 8.99 (d, *J* = 7.8 Hz, 1H, 3), 8.83 (d, *J* = 8.2 Hz, 2H, T_3', T_5'), 8.64 (d, *J* = 8.1 Hz, 2H, T_6, T_6''), 8.51 (d, *J* = 8.3 Hz, 1H, 10), 8.48 – 8.43 (m, 2H, T_4', 2), 8.40 (d, *J* = 8.9 Hz, 1H, 5), 8.21 (d, *J* = 8.9 Hz, 1H, 6), 8.05 (td, *J* = 8.0, 1.9 Hz, 2H, T_5'', T_5), 7.73 – 7.68 (m, 1H, 8), 7.65 (d, *J* = 5.4 Hz, 2H, T_3", T_3), 7.58 (dd, *J* = 8.2, 5.3 Hz, 1H, 9), 7.35 – 7.28 (m, 2H, T_4, T_4"), 4.29 (d, *J* = 7.7 Hz, 1H, H-1), 4.04 – 3.96 (m, 1H, C*H*H H-6), 3.90 – 3.83 (m, 1H, C*H*H OCH_2), 3.74 – 3.47 (m, 10H, C*H*H H-6, C*H*H OCH_2, 4 x O*C*H_2), 3.37 (m, 1H, H-5), 3.30 – 3.25 (m, 2H, H-3, H-4), 3.14 (dd, *J* = 9.0, 7.9 Hz, 1H, H-2), 2.02 (t, *J* = 5.5 Hz, 2H, O*C*H_2SMe), 1.51 (s, 3H, OCH_2S*Me*). ^{13}C NMR (101 MHz, CD_3OD) δ = 159.4 (C_q Arom), 158.9 (C_q Arom), 154.5 (C_H T_3'', T_3), 154.3 (C_H 1), 151.7 (C_H 8), 148.6 (C_q Arom), 148.2 (C_q Arom), 140.0 (C_H T_5", T_5), 138.6 (C_H 3), 138.4 (C_H 10, 2), 132.9 (C_q Arom), 132.0 (C_q Arom), 129.7 (C_H 5, T_4, T_4"), 128.9 (C_H 6), 127.9 (C_H T_4'), 126.8 (C_H 9), 126.2 (C_H 10, T_6, T_6"), 125.5 (C_H T_3', T_5'), 104.4 (C-1), 77.8 (C-3, C-5), 75.1 (C-2), 71.6 (C-4), 71.4 (O*C*H_2), 71.3 (O*C*H_2), 71.1 (O*C*H_2), 69.7 (C-6), 68.4 (O*C*H_2), 62.7 (O*C*H_2), 35.7 (O*C*H_2SMe), 15.6 (O*C*H_2S*Me*). HRMS: m/z calcd for $[C_{40}H_{45}O_8N_5RuS\ P_2F_{12} - 2PF_6]^{2+}$: 428.60107, found: 428.60248. Elemental analysis calcd (%) for [**2b**]$(PF_6)_2$: C, 41.89; H, 3.96; N, 6.11; found: C, 41.81; H, 4.03; N, 6.07.

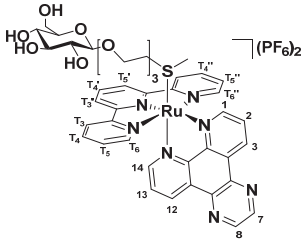

[Ru(tpy)(dpq)(R)]$(PF_6)_2$, [3b]$(PF_6)_2$: A mixture of [Ru(tpy)(dpq)Cl]Cl (75.0 mg, 0.118 mmol) and 2-(2-(2-(methylthio)ethoxy)ethoxy)ethyl-β-D-glucopyranoside (63 mg, 0.184) in deoxygenated H_2O (20 mL) were stirred at 80 °C for 48 h and concentrated *in vacuo*. The crude was redissolved in H_2O (20 mL) and $AgPF_6$ (71 mg, 0.281 mmol) and 2-(2-(2-(methylthio)ethoxy)ethoxy)ethyl-β-D-glucopyranoside (63 mg, 0.184 mmol) were added. After stirring for another 16 h at 80 °C, the mixture was hot filtered over Celite® and concentrated *in vacuo*. The crude was further purified over silica (acetone/water/sat. KPF_6, 100/0/0 - 100/80/20) by collection of the orange fraction. Excess KPF_6 was then removed using a Sephadex LH-20 column (MeOH), yielding [**3b**]$(PF_6)_2$ as a dark orange solid. (33.0 mg, 0.0301 mmol, 25%). R_f = 0.55 (acetone/water/sat. KPF_6, 100/80/20); ^{1}H NMR (400 MHz, CD_3OD) δ = 10.26 (d, *J* = 5.2 Hz, 1H, 1), 9.97 (d, *J* = 8.3 Hz, 1H, 3), 9.50 (d, *J* = 8.2 Hz, 1H, 14), 9.29 (d, *J* = 2.4 Hz, 1H, 7), 9.22 (d, *J* = 2.4 Hz, 1H, 8), 8.86 (d, *J* = 8.2 Hz, 2H, T_3', T_5'), 8.68 (d, *J* = 8.1 Hz, 2H, T_6, T_6"), 8.60 (dd, *J* = 8.5, 5.1 Hz, 1H, 2), 8.48 (t, *J* = 8.1 Hz, 1H, T_4'), 8.07 (t, *J* = 7.9 Hz, 2H, T_5", T_5), 7.81 (d, *J* = 5.7 Hz, 1H, 12), 7.77 (d, *J* = 5.5 Hz, 2H, T_3, T_3"), 7.72 (dd, *J* = 8.5, 5.2 Hz, 1H, 13), 7.34 (t, *J* = 6.6 Hz, 2H, T_4, T_4"), 4.26 (d, *J* = 7.8 Hz, 1H, H-1), 4.06 – 3.94 (m, 1H, C*H*H H-6), 3.85 (d, *J* = 11.8 Hz, 1H, C*H*H OCH_2), 3.76 – 3.46 (m, 10H, C*H*H H-6, C*H*H OCH_2, 4 x O*C*H_2), 3.35

(m, 1H, H-5), 3.27 – 3.18 (m, 2H, H-3, H-4), 3.08 (t, *J* = 8.5 Hz, 1H, H-2), 2.03 (t, *J* = 5.4 Hz, 2H, OC*H*$_2$SMe), 1.51 (s, 3H, OCH$_2$S*Me*). ^{13}C NMR (101 MHz, CD_3OD) δ = 159.3 (C_q Arom), 158.9 (C_q Arom), 155.3 (C_H 1), 154.8 (C_H T_3, T_3"), 152.9 (C_H 12), 150.3 (C_q Arom), 150.0 (C_q Arom), 148.0 (C_H 7), 147.9 (C_H 8), 141.2 (C_q Arom), 140.8 (C_q Arom), 140.2 (C_H T_5", T_5), 138.5 (C_H T_4'), 135.2 (C_H 3), 135.0 (C_H 14), 132.0 (C_q Arom), 131.1 (C_q Arom), 129.8 (C_H T_4, T_4"), 128.8 (C_H 2), 127.7 (C_H T_3, T_3"), 126.3 (C_H T_6, T_6"), 125.5 (C_H T_3', T_5), 111.8 (C_q Arom), 111.4 (C_q Arom), 104.5 (C-1), 78.0 (C-3, C-5), 75.1 (C-2), 71.6 (C-4), 71.4 (O*C*H$_2$), 71.3 (O*C*H-$_2$), 71.2 (O*C*H$_2$), 69.7 (C-6), 68.4 (O*C*H$_2$), 62.7 (O*C*H$_2$), 35.8 (O*C*H$_2$SMe), 15.5 (O*C*H$_2$S*Me*). HRMS: m/z calcd for $[C_{40}H_{45}O_8N_5RuSP_2F_{12} - 2PF_6]^{2+}$: 454.60414, found: 454.60602; Elemental analysis calcd (%) for [**3b**]$(PF_6)_2$.5H_2O: C, 39.14; H, 4.30; N, 7.61; found: C, 40.32; H, 4.28; N, 7.20.

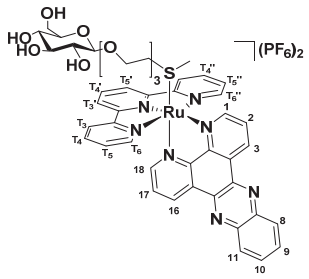

[Ru(tpy)(dppz)(R)]$(PF_6)_2$, [4b]$(PF_6)_2$: [Ru(tpy)(dppz)Cl]Cl (67 mg, 0.097 mmol) and 2-(2-(2-(methylthio)ethoxy)ethoxy)ethyl-β-D-glucopyranoside (50.0 mg, 0.146 mmol) were dissolved in deoxygenated H_2O (16 mL) and the reaction was heated at 80 °C under an inert atmosphere overnight. KPF_6 (~200 mg) was added, the mixture was concentrated *in vacuo* at 37 °C in the dark, followed by purification of the crude over silica (acetone/water/sat. KP_6, 100% - 50/50/0 - 100/80/20). The orange band was collected, and excess KPF_6 was removed *via* Sephadex LH-20 (MeOH) purification. Removal of the solvent under reduced pressure yielded the title compound as a dark red solid (32.0 mg, 0.026 mmol, 26%). R_f = 0.56 (100/80/20 acetone/water/sat. KPF_6); ^{1}H NMR (400 MHz, CD_3OD) δ = 10.25 (d, *J* = 1.3 Hz, 1H, 1), 10.08 (d, *J* = 8.2 Hz, 1H, 3), 9.60 (d, *J* = 6.7 Hz, 1H, 18), 8.86 (d, *J* = 8.1 Hz, 2H, T_3', T_5'), 8.68 (d, *J* = 8.0 Hz, 2H, T_6", T_6), 8.63 – 8.54 (m, 2H, 2, 11), 8.52 – 8.40 (m, 2H, T_4', 8), 8.19 – 8.03 (m, 4H, 9, 10, T_5, T_5"), 7.86 – 7.80 (m, 2H, T_3, T_3"), 7.78 (dd, *J* = 5.4, 1.5 Hz, 2H, 16), 7.71 (dd, *J* = 8.1, 5.4 Hz, 2H, 17), 7.36 (t, *J* = 6.6 Hz, 2H, T_4, T_4"), 4.26 (d, *J* = 7.7 Hz, 1H, H-1), 4.07 – 3.94 (m, 1H, C*H*H H-6), 3.85 (d, *J* = 11.7 Hz, 1H, C*H*H OCH$_2$), 3.74 – 3.48 (m, 10H, C*H*H H-6, C*H*H OCH$_2$, 4 x O*CH*$_2$), 3.25 – 3.21 (m, 2H, H-3, H-4), 3.17 (d, *J* = 3.0 Hz, 1H, H-5), 3.10 (dd, *J* = 9.0, 7.8 Hz, 1H, H-2), 2.03 (t, *J* = 5.4 Hz, 2H, OC*H*$_2$SMe), 1.50 (s, 3H, OCH$_2$S*Me*). ^{13}C NMR (101 MHz, CD_3OD) δ = 159.3 (C_q Arom), 158.9 (C_q Arom), 155.2 (C_H 1), 154.9 (C_H T_3, T_3"), 152.8 (C_H 17), 151.4 (C_q Arom), 144.4 (C_q Arom), 144.0 (C_q Arom), 141.4 (C_q Arom), 141.0 (C_q Arom), 140.2 (C_H T_5, T_5"), 138.5 (C_H 8), 135.5 (C_H 3), 135.3 (C_H 18), 133.5 (C_H 9), 133.5 (C_H 10), 130.9 (C_H T_4'), 130.8 (C_H 2), 129.8 (C_H T_4, T_4"), 129.0 (C_H 11), 128.0 (C_H 17), 126.3 (C_H T_6", T_6), 125.5 (C_H T_3', T_5'), 104.5 (C-1), 78.0 (C-3, C-5), 75.1 (C-2), 71.6 (C-4), 71.4 (O*C*H$_2$), 71.4 (O*C*H$_2$), 71.2 (O*C*H$_2$), 69.7 (C-6), 68.4 (O*C*H$_2$), 62.7 (O*C*H$_2$), 35.8 (O*C*H$_2$SMe), 15.5 (O*C*H$_2$S*Me*). HRMS: m/z calcd for $[C_{46}H_{47}O_8N_7RuSP_2F_{12} - 2PF_6]^{2+}$: 479.61197; found: 479.61362; Elemental analysis calcd (%) for [**4b**]$(PF_6)_2$.6H_2O: C, 40.71; H, 4.38; N 7.23; found: C, 40.32; H, 4.28; N, 7.20.

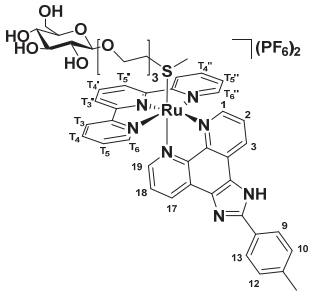

[Ru(tpy)(pmip)(R)](PF$_6$)$_2$, [6b](PF$_6$)$_2$: $AgNO_3$ (0.152 g, 0.895 mmol) was added to a solution of [Ru(tpy)(pmip)Cl]Cl (0.251 g, 0.351 mmol) in acetone/H_2O (60 mL, 3:1). The resulting mixture was heated overnight at 50 °C under an inert atmosphere and then hot-filtered over Celite®. The volume was reduced (~10%), 2 mL saturated aqueous NH_4PF_6 was added, and the resulting brown precipitate was collected on a glass frit, washed with H_2O (3 x 50 mL) and Et_2O (3 x 50 mL) affording the title compound as a brown powder which was used without further purification. (0.275 g, 0.215 mmol, 95%). An aliquot (60.0 mg, 0.0630 mmol) was then, together with 2-(2-(2-(methylthio)ethoxy)ethoxy)ethyl-β-L-glucopyranoside (40.0 g, 0.117 mmol) dissolved in deoxygenated acetone (11 mL) and stirred at 50 °C under an inert atmosphere overnight in the dark, followed by concentration under vacuum at 30 °C in the dark and purification over a Sephadex LH-20 column (MeOH). The orange fraction was collected and the volume was reduced to ~10% then Et_2O was added. The resulting precipitate was collected by filtration on a Whatman® RC60 membrane filter, then washed with EtOAc (3 x 50 mL), Et_2O (3 x 50 mL) and heptane (3 x 50 mL) affording [**6b**](PF$_6$)$_2$ as an orange powder (60 mg, 0.047 mmol, 75%). R_f = 0.48 (100/80/20 acetone/water/sat. KPF_6); ^{1}H NMR (500 MHz, [D$_6$]acetone) δ = 10.21 (d, *J* = 5.2 Hz, 1H, 1), 9.44 (d, *J* = 8.2 Hz, 1H, 2), 8.99 (d, *J* = 8.2 Hz, 2H, T$_3$', T$_5$'), 8.90 (d, *J* = 8.2 Hz, 1H, 21), 8.79 (d, *J* = 8.0 Hz, 2H, T$_3$, T$_3$"), 8.60 – 8.52 (m, 2H, 2, T$_4$'), 8.22 (d, *J* = 8.2 Hz, 2H, 9, 13), 8.18 – 8.09 (m, 2H, T$_4$, T$_4$"), 7.97 (d, *J* = 5.4 Hz, 2H, T$_6$, T$_6$"), 7.83 (d, *J* = 5.4 Hz, 1H, 19), 7.61 (dd, *J* = 8.2, 5.2 Hz, 1H, 20), 7.46 – 7.35 (m, 4H, T$_3$, T$_3$", 10, 12), 4.31 (d, *J* = 7.7 Hz, 1H, H-1), 3.99 – 3.89 (m, 1H, C*H*H H-5), 3.84 (dd, *J* = 11.7, 2.7 Hz, 1H, C*H*H OCH$_2$), 3.72 – 3.48 (m, 10H, C*H*H H-6, C*H*H OCH$_2$, 4 x OC*H$_2$*), 3.43 – 3.22 (m, 2H, H-3, H-4, H-5), 3.13 (t, *J* = 8.3 Hz, 1H, H-2), 2.42 (s, 3H, CH$_3$ Tol), 2.21 (t, *J* = 5.4 Hz, 2H), 1.63 (s, 3H, OCH$_2$S*Me*). ^{13}C NMR (126 MHz, (CD$_3$)$_2$CO) δ = 159.0 (C$_q$ Arom), 158.6 (C$_q$ Arom), 154.8 (C$_H$ T$_6$, T$_6$"), 154.4 (C$_q$ Arom), 151.8 (C$_H$ 1), 149.3 (C$_H$ 19), 146.3 (C$_q$ Arom), 146.0 (C$_q$ Arom), 141.5 (C$_q$ Arom), 139.7 (C$_H$ T$_4$, T$_4$"), 137.9 (C$_H$ 2), 131.9 (C$_H$ 3), 131.6 (C$_H$ 21), 130.6 (C$_H$ T$_5$, T$_5$"), 129.5 (C$_H$ 10, 12), 127.9 (C$_q$ Arom), 127.5 (C$_H$ 9, 13, T$_4$'), 126.3 (C$_H$ 20), 125.9 (C$_H$ T$_3$, T$_3$"), 125.2 (C$_H$ T$_3$', T$_3$'), 104.2 (C-1), 78.0 (C-3), 77.5 (C-5), 74.8 (C-2), 71.6 (C-4), 71.3 (O*C*H$_2$), 71.0 (O*C*H$_2$), 70.9 (O*C*H$_2$), 69.2 (C-6), 68.2 (O*C*H$_2$), 62.8 (O*C*H$_2$), 35.8 (O*C*H$_2$), 21.4 (CH$_3$ Tol), 15.6 (O*C*H$_2$SMe). HRMS: m/z calcd for $[C_{48}H_{51}O_8N_7RuSP_2F_{12} - 2PF_6]^{2+}$: 493.62762, found: 493.62791; Elemental analysis calcd (%) for [**6b**](PF$_6$)$_2$: C, 45.15; H, 4.03; N, 7.68; found: C, 45.35; H, 4.23; N, 7.53.

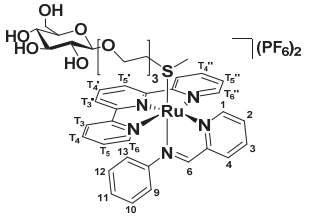

[Ru(tpy)(pymi)(R)](PF$_6$)$_2$, [7b](PF$_6$)$_2$: [Ru(tpy)(pymi)Cl]Cl (30.0 mg, 0.0429 mmol) and 2-(2-(2-(methylthio)ethoxy)ethoxy)ethyl-β-D-glucopyranoside (83.0 mg, 0.242 mmol) were dissolved in acetone/H_2O (1:1, 7 mL) and to this mixture was added $AgPF_6$ (31 mg, 0.123 mmol).

After stirring for 72 h at reflux under inert atmosphere in the dark, the mixture was filtered over Celite® and concentrated *in vacuo* in the dark at 30 °C. The crude was then purified over silica (acetone/water/sat. KPF_6 100/0/0 - 100/80/20) collecting the orange fraction. Subsequent purification over Sephadex LH-20 (MeOH) afforded, after concentrating *in vacuo* the title compound as an orange paste (19 mg, 0.016 mmol, 37%). R_f = 0.64 (100/80/20 acetone/water/sat. KPF_6). ^{1}H NMR (400 MHz, CD_3OD) δ = 9.85 (d, *J* = 5.5 Hz, 1H, 1), 8.89 (s, 1H, 6), 8.59 – 8.51 (m, 3H, 3, T_3, T_3''), 8.45 (d, *J* = 8.2 Hz, 3H, T_3', T_5', 4), 8.21 (t, *J* = 8.1 Hz, 3H, 2, T_4, T_4''), 8.09 (t, *J* = 8.1 Hz, 1H, T_4'), 7.85 (d, *J* = 5.4 Hz, 2H, T_6'', T_6), 7.69 – 7.59 (m, 2H, T_5, T_5''), 7.11 (t, *J* = 7.5 Hz, 1H, 11), 6.96 (t, *J* = 7.7 Hz, 2H, 9, 13), 5.79 (d, *J* = 7.9 Hz, 2H, 10, 12), 4.25 (d, *J* = 7.8 Hz, 1H, H-1), 3.98 (m, 1H, C*H*H H-6), 3.86 (d, *J* = 11.7 Hz, 1H, C*H*H OCH2), 3.73 – 3.38 (m, 10H, C*H*H H-6, C*H*H OCH_2, 4 x O*C*H_2), 3.34 (d, *J* = 4.0 Hz, 1H), 3.24 (d, *J* = 6.6 Hz, 1H), 3.12 – 3.04 (m, 1H, H-5), 1.94 (t, *J* = 5.4 Hz, 2H, O*C*H_2SMe), 1.42 (s, 3H, OCH_2S*Me*). ^{13}C NMR (101 MHz, CD_3OD) δ = 170.9 (C_H 6), 159.3 (C_q Arom), 158.1 (C_q Arom), 157.9 (C_q Arom), 155.1 (C_H T_6'', T_6), 153.9 (C_H 1), 140.5 (C_H T_4, T_4''), 139.1 (C_H 4), 137.9 (C_H T_4'), 132.4 (C_H 3), 130.8 (C_H 2), 130.3 (C_H 9, 13), 130.2 (C_H T_5, T_5''), 129.2 (C_H 11), 125.9 (C_H T_3, T_3''), 124.8 (C_H T_3', T_5'), 120.9 (C_H 10, 12), 104.5 (C-1), 78.0 (C-3, C-5), 75.1 (C-2), 71.6 (C-4), 71.4 (O*C*H_2), 71.3 (O*C*H_2), 71.2 (O*C*H_2), 69.7 (C-6), 68.4 (O*C*H_2), 62.7 (O*C*H_2), 35.8 (O*C*H_2SMe), 15.7 (O*C*H_2SMe). HRMS: m/z calcd for $[C_{40}H_{47}O_8N_5RuSP_2F_{12} – 2PF_6]^{2+}$: 429.60889, found: 429.61047.

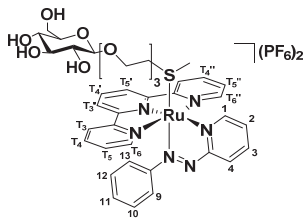

[Ru(tpy)(azpy)(R)](PF$_6$)$_2$, [8b](PF$_6$)$_2$: [Ru(tpy)(azpy)Cl]Cl (47.0 mg, 0.0849 mmol) and 2-(2-(2-(methylthio)ethoxy)ethoxy)ethyl-β-D-glucopyranoside (50.0 mg, 0.146 mmol) were dissolved in deoxygenated H_2O (5 mL, 0.02 M) and stirred at 80 °C for 48 h under an inert atmosphere after which solvents were removed under reduced pressure at 30 °C in the dark. The crude was then purified over silica (acetone/water/sat. KPF_6 100/0/0 - 100/80/20) by collection of the light purple fraction. Subsequent purification over Sephadex LH-20 (MeOH) afforded [**8b**](PF$_6$)$_2$ as a purple solid (15 mg, 0.013 mmol, 15%). *Rf* = 0.34 (acetone/water/sat. KPF_6 100/80/20); ^{1}H NMR (400 MHz, CD_3OD) δ = 9.75 (d, *J* = 5.6 Hz, 1H, 1), 9.02 (d, *J* = 8.0 Hz, 1H, 4), 8.59 (d, *J* = 8.1 Hz, 5H, T_3', T_5', T_6, T_6''), 8.36 – 8.27 (m, 2H, 2, T_5''), 8.27 – 8.18 (m, 2H, T_5, T_4'), 7.63 – 7.57 (m, 4H, T_3'', T_3, T_4'', T_4), 7.28 (t, *J* = 7.5 Hz, 1H, 11), 7.07 (t, *J* = 7.9 Hz, 2H, 10, 12), 6.20 (d, *J* = 7.5 Hz, 2H, 9, 13), 4.26 (d, *J* = 7.8 Hz, 1H, H-1), 4.02 – 3.94 (m, 1H, C*H*H H-6), 3.89 – 3.82 (m, 1H, O*CH*H), 3.72 – 3.45 (m, 10H, C*H*H H-6, O*CH*H, 4 x O*C*H_2), 3.38 – 3.30 (m, 1H, H-5), 3.27 – 3.21 (m, 2H, H-3, H-4), 3.09 (t, *J* = 8.4 Hz, 1H, H-2), 2.02 (t, *J* = 5.4 Hz, 2H, O*C*H_2SMe), 1.50 (s, 3H, CH_3 OCH_2S*Me*). ^{13}C NMR (101 MHz, CD_3OD) δ = 167.2 (C_q Arom), 158.7 (C_q Arom), 156.9 (C_q Arom), 155.1 (C_H T_4'', T_4), 151.6 (C_H 1), 141.7 (C_H T_4', T_5), 141.1 (C_H 3), 139.7 (C_H 2), 131.4 (C_H 11), 130.8 (C_H 4), 130.5 (C_H 10, 2), 130.3 (C_H T_3'', T_3), 126.6 (C_H T_6, T_6''), 125.7 (C_H T_3', T_5'), 121.4 (C_H 9, 13), 111.4 (C_q Arom), 104.4 (C-1), 78.0 (C-3, C-5), 75.1

(C-2), 71.6 (C-4), 71.4 (O*C*H_2), 71.3 (O*C*H_2), 71.2 (O*C*H_2), 69.7 (C-6), 68.2 (O*C*H_2), 62.7 (O*C*H_2), 36.1 (O*C*H_2SMe), 15.7 (O*C*H_2S*Me*). HRMS: m/z calcd for [$C_{39}H_{46}O_8N_6RuSP_2F_{12}$ – 2PF_6]: 430.10652, found: 430.10721. Elemental analysis calcd (%) for [**8b**](PF_6)$_2$: C, 40.74; H 4.03; N, 7.31; found: C, 40.53; H, 3.99; N, 7.15.

4.5.3 Photochemistry

4.5.3.1 General

Irradiation experiments were performed using a quartz fluorescence cuvette (1 cm path length) irradiated from the top (3 cm optical pathlength) with a custom-built LED light source equipped with either a Roithner LaserTechnik H2A1-H450 LED (λ_{exc} 450 nm, FWHM 35 nm) or H2A1-H470 LED (λ_{exc} 470 nm, FWHM 35 nm). UV-vis spectra were recorded on an Agilent Cary® 50 UV–vis spectrometer equipped with a Cary Single Cell Peltier and accessory for temperature control. Photon fluxes for both LEDs were determined using standard ferrioxalate actinometry.[36]

4

4.5.3.2 Photosubstitution quantum yield measurements

General procedure: 3.00 mL of a solution of [**1b**](PF_6)$_2$ ($1.38 \cdot 10^{-4}$ M) in H_2O was deoxygenated for 15 minutes with dinitrogen gas, after which it was irradiated at constant temperature (25 °C). During irradiation UV-vis spectra were recorded on a Varian Inc. Cary 50 UV-vis spectrometer with intervals of 30 seconds until t = 3600 seconds. ESI-MS spectra were recorded after the irradiation experiment to confirm the formation of the aqua species $[Ru(tpy)(bpy)(OH_2)]^{2+}$ (m/z 254.5 calculated, 254.6 found). The quantum yield for the photosubstitution of the thioether ligand was calculated according to the method described earlier.[37] Reference molar absorption coefficients used to calculate concentrations during irradiation are provided in table 4.4.

Table 4.4. Reference wavelengths (λ_{ref}) and molar absorption coefficients (ε_{ref}) for photosubstitution quantum yield calculations. RuSRR' = [Ru(tpy)(NN)(2-(2-(2-(methylthio)ethoxy)ethoxy)ethyl-β-D-glucopyranoside)](PF_6)$_2$ $RuOH_2$ = [Ru(tpy)(N-N)H_2O](PF_6)$_2$.

Compound	$\lambda_{ref\ in\ nm}$	ε_{ref} RuSRR' (M^{-1} cm^{-1})	ε_{ref} $RuOH_2$ (M^{-1} cm^{-1})	N-N
[1b](PF_6)$_2$	490	8.5×10^3	3.0×10^3	bpy
	410	3.1×10^3	5.0×10^3	
[2b](PF_6)$_2$	490	2.1×10^3	8.3×10^3	phen
	410	5.2×10^3	5.7×10^3	
[3b](PF_6)$_2$	490	3.9×10^3	6.7×10^3	dpq
	410	7.0×10^3	3.6×10^3	
[4b](PF_6)$_2$	490	7.5×10^3	4.4×10^3	dppz
	420	4.8×10^3	7.2×10^3	
[5b](PF_6)$_2$	490	7.4×10^3	12.4×10^3	dppn
	430	10.5×10^3	10.8×10^3	
[6b](PF_6)$_2$	490	4.5×10^3	14.1×10^3	pmip
	430	8.9×10^3	6.6×10^3	
[7b](PF_6)$_2$	490	8.7×10^3	14.0×10^3	pymi
	410	4.1×10^3	2.7×10^3	

4.5.3.3 Singlet oxygen and phosphorescence quantum yield

Emission measurements were carried out as described in appendix I.1.1.

4.5.4 Cytotoxicity Assay

The cytotoxicity assay was carried out as described in appendix I.2.1 with compounds [**1a**]Cl – [**8a**]Cl and [**1b**]$(PF_6)_2$ – [**8a**]$(PF_6)_2$. All compounds were dissolved in OMEM with the exception of [**4a**]Cl, [**5a**]Cl and [**6a**]Cl for which (a maximum of 0.5%) DMSO was used.

4.5.6 Cellular uptake

A549 cells were seeded (3 x 10^5) in a volume of 3 mL OptiMEM in 6-well plates. After 24 h 1 mL of a 100 μM stock solution of [**1a**]Cl-[**8a**]Cl and [**1b**]$(PF_6)_2$-[**8b**]$(PF_6)_2$ in OMEM was added and incubated for 24 h. After 24 h incubation, the media was removed and the wells were washed with PBS (2 x 2 mL). Cells were trypsinized (1 mL) at 37 °C and transferred to a 14 mL corning tube with OMEM (2 x 2 mL). Corning tubes were centrifuged (1.2 RCF, 4 minutes). Media was aspirated and pellets were re-suspended in 1 mL PBS, and cells were counted. Samples were then centrifuged again, and the resulting pellets transferred to 10 mL glass vials with MilliQ (2 x 100 μL), followed by overnight digestion with 2 mL 65% HNO_3. Aliquots of 1 mL were then diluted to 14 mL using MilliQ in 15 mL corning tubes. Ruthenium concentrations in each sample were then determined using ICP-MS. ICP-MS measurements were carried out on a i-CAP-Q ICP-MS (Thermo Scientific, Walthem, Massachusetts, USA). The system was optimized with a ruthenium-platinum solution which was calibrated within the range 0 - 25 μg/L, with a detection limit of 0.01 μg/L for all isotopes. Silver and Indium were used as an internal standard, to correct for sample dependent matrix effects. No reference sample was available; therefore several samples were spiked with a known concentration. The recovery of the spiked concentrations were all within a 10% deviation.

4.5.7 Log $P_{o/w}$ determination

The partition coefficient between *n*-octanol and water (Log $P_{o/w}$) were determined according to the procedure described in appendix I.1.2.3: Stock solutions of complexes [**1a**]Cl - [**8a**]Cl and [**1b**]$(PF_6)_2$ - [**8b**]$(PF_6)_2$ (1 x 10^{-3} M) were prepared by dissolving the compounds in *n*-octanol saturated MilliQ water and [**4a**]Cl, [**5a**]Cl, [**6a**]Cl were dissolved in MilliQ saturated *n*-octanol water. For [**4a**] – [**6a**]Cl stock solution concentrations could not be determined *via* ICP-OES. These concentrations were calculated.

Log P values for [**1a/b-8a/b**]Cl/$(PF_6)_2$. SD = Standard deviation. Experiments were carried out in triplicate.

Compound	Mean	SD
[**1a**]Cl	-1.12	0.15
[**2a**]Cl	-1.08	0.16
[**3a**]Cl	-0.81	0.07
[**4a**]Cl	-0.02	0.01
[**5a**]Cl	1.01	0.04
[**6a**]Cl	-0.10	0.04
[**7a**]Cl	-1.61	0.19
[**8a**]Cl	-1.81	0.24
[**1b**]$(PF_6)_2$	-0.23	0.08
[**2b**]$(PF_6)_2$	-0.12	0.04
[**3b**]$(PF_6)_2$	-0.51	0.02
[**4b**]$(PF_6)_2$	-0.84	0.08
[**5b**]$(PF_6)_2$	-0.50	0.13
[**6b**]$(PF_6)_2$	-0.84	0.19
[**7b**]$(PF_6)_2$	-0.20	0.02
[**8b**]$(PF_6)_2$	-0.18	0.01

4.5.8 Crystals

Single crystals of [**3a**]$(PF_6)_2$, [**4a**]$(PF_6)_2$ and [**5a**]Cl were obtained as follows: [**3a**]Cl and [**4a**]Cl were converted to their corresponding PF_6 salts by dissolving them in a minimum amount of MeOH and adding a saturated solution of NH_4PF_6 in H_2O, the resulting precipitates were washed with H_2O (3x) and Et_2O (3x) and dissolved in 0.5 mL acetone in a small mass vial (~1 mg · mL^{-1}) and placed in a larger vial containing ~3 mL Et_2O (for [**3b**]$(PF_6)_2$) or ~3 mL EtOAc (for [**4b**]$(PF_6)_2$). A similar approach, but without the counter-anion exchange, was used for [**5a**]Cl with diisopropylether in acetonitrile. Detailed crystallographic data is provided in appendix III.1.

References

[1] a). Z. Adhireksan, G. E. Davey, P. Campomanes, M. Groessl, C. M. Clavel, H. Yu, A. A. Nazarov, C. H. Yeo, W. H. Ang, P. Droge, U. Rothlisberger, P. J. Dyson, C. A. Davey, *Nat Commun* **2014**, *5*, 3462; b). M. H. Seelig, M. R. Berger, B. K. Keppler, *J Cancer Res Clin Oncol* **1992**, *118*, 195-200; c). M. Colucci, M. Coluccia, P. Montemurro, M. Conese, A. Nassi, F. Loseto, E. Alessio, G. Mestroni, N. Semeraro, *Int J Oncol* **1993**, *2*, 527-529; d). O. Novakova, J. Kasparkova, O. Vrana, P. M. Vanvliet, J. Reedijk, V. Brabec, *Biochemistry* **1995**, *34*, 12369-12378; e). A. C. G. Hotze, H. Kooijman, A. L. Spek, J. G. Haasnoot, J. Reedijk, *New J Chem* **2004**, *28*, 565-569.

[2] A.-M. Florea, D. Büsselberg, *Cancers* **2011**, *3*, 1351-1371.

[3] a). S. Leijen, S. A. Burgers, P. Baas, D. Pluim, M. Tibben, E. van Werkhoven, E. Alessio, G. Sava, J. H. Beijnen, J. H. Schellens, *Invest New Drugs* **2015**, *33*, 201-214; b). C. Mari, V. Pierroz, S. Ferrari, G. Gasser, *Chem Sci* **2015**, *6*, 2660-2686.

[4] G. Subramanian, P. Parakh, H. Prakash, *Photobiol Sci* **2013**, *12*, 456-466.

[5] K. Davia, D. King, Y. L. Hong, S. Swavey, *Inorg Chem Commun* **2008**, *11*, 584-586.

[6] J. Fong, K. Kasimova, Y. Arenas, P. Kaspler, S. Lazic, A. Mandel, L. Lilge, *Photobiol Sci* **2015**, *14*, 2014-2023.

[7] L. M. Loftus, J. K. White, B. A. Albani, L. Kohler, J. J. Kodanko, R. P. Thummel, K. R. Dunbar, C. Turro, *Chem Eur J* **2016**.

[8] L. Zayat, C. Calero, P. Albores, L. Baraldo, R. Etchenique, *J Am Chem Soc* **2003**, *125*, 882-883.

[9] a). M. A. Sgambellone, A. David, R. N. Garner, K. R. Dunbar, C. Turro, *J Am Chem Soc* **2013**, *135*, 11274-11282; b). R. N. Garner, J. C. Gallucci, K. R. Dunbar, C. Turro, *Inorg Chem* **2011**, *50*, 9213-9215.

[10] T. Joshi, V. Pierroz, C. Mari, L. Gemperle, S. Ferrari, G. Gasser, *Angew Chem Int Ed* **2014**, *53*, 2960-2963.

[11] E. Wachter, D. K. Heidary, B. S. Howerton, S. Parkin, E. C. Glazer, *Chem Commun* **2012**, *48*, 9649-9651.

[12] a). M. K. Herroon, R. Sharma, E. Rajagurubandara, C. Turro, J. J. Kodanko, I. Podgorski, *Biol Chem* **2016**, *397*, 571-582; b). A. Li, R. Yadav, J. K. White, M. K. Herroon, B. P. Callahan, I. Podgorski, C. Turro, E. E. Scott, J. J. Kodanko, *Chem Commun* **2017**, *53*, 3673-3676.

[13] a). V. H. S. van Rixel, B. Siewert, S. L. Hopkins, S. H. C. Askes, A. Busemann, M. A. Siegler, S. Bonnet, *Chem Sci* **2016**, *7*, 4922-4929; b). L. N. Lameijer, S. L. Hopkins, T. G. Breve, S. H. Askes, S. Bonnet, *Chem Eur J* **2016**, *22*, 18484-18491.

[14] a). B. Siewert, V. H. van Rixel, E. J. van Rooden, S. L. Hopkins, M. J. Moester, F. Ariese, M. A. Siegler, S. Bonnet, *Chem Eur J* **2016**, *22*, 10960-10968; b). R. E. Goldbach, I. Rodriguez-Garcia, J. H. van Lenthe, M. A. Siegler, S. Bonnet, *Chem Eur J* **2011**, *17*, 9924-9929.

[15] O. Novakova, J. Kasparkova, O. Vrana, P. M. van Vliet, J. Reedijk, V. Brabec, *Biochemistry* **1995**, *34*, 12369-12378.

[16] A. Mijatovic, B. Smit, A. Rilak, B. Petrovic, D. Canovic, Z. D. Bugarcic, *Inorg Chim Acta* **2013**, *394*, 552-557.

[17] S. Bonnet, J. P. Collin, N. Gruber, J. P. Sauvage, E. R. Schofield, *Dalton Trans* **2003**, 4654-4662.

[18] A. K. Martensson, P. Lincoln, *Dalton Trans* **2015**, *44*, 3604-3613.

[19] A. C. Hotze, J. A. Faiz, N. Mourtzis, G. I. Pascu, P. R. Webber, G. J. Clarkson, K. Yannakopoulou, Z. Pikramenou, M. J. Hannon, *Dalton Trans* **2006**, 3025-3034.

[20] A. E. M. Boelrijk, A. M. J. Jorna, J. Reedijk, *J Mol Catal Chem* **1995**, *103*, 73-85.

[21] A. Bahreman, B. Limburg, M. A. Siegler, E. Bouwman, S. Bonnet, *Inorg Chem* **2013**, *52*, 9456-9469.

[22] a). K. Hansongnern, U. Saeteaw, G. Mostafa, Y. C. Jiang, T. H. Lu, *Anal Sci* **2001**, *17*, 683-684; b). F. N. Rein, W. Chen, B. L. Scott, R. C. Rocha, *Acta Crystallogr E Crystallogr Commun* **2015**, *71*, 1017-1021.

[23] a). B. A. Albani, C. B. Durr, C. Turro, *J Phys Chem A* **2013**, *117*, 13885-13892; b). J. D. Knoll, B. A. Albani, C. Turro, *Chem Commun* **2015**, *51*, 8777-8780.

[24] V. Vichai, K. Kirtikara, *Nat Protocols* **2006**, *1*, 1112-1116.

[25] E. Corral, A. C. Hotze, H. den Dulk, A. Leczkowska, A. Rodger, M. J. Hannon, J. Reedijk, *J Biol Inorg Chem* **2009**, *14*, 439-448.

[26] U. Schatzschneider, J. Niesel, I. Ott, R. Gust, H. Alborzinia, S. Wolfl, *ChemMedChem* **2008**, *3*, 1104-1109.

[27] A. P. Castano, T. N. Demidova, M. R. Hamblin, *Photodiagnosis Photodyn Ther* **2004**, *1*, 279-293.

[28] Oecd, *OECD Guidelines for the Testing of Chemicals*, The Organisation for Economic Co-operation and Development, **1994**.

[29] M. Frasconi, Z. Liu, J. Lei, Y. Wu, E. Strekalova, D. Malin, M. W. Ambrogio, X. Chen, Y. Y. Botros, V. L. Cryns, J.-P. Sauvage, J. F. Stoddart, *J Am Chem Soc* **2013**, *135*, 11603-11613.

[30] E. B. van der Tol, H. J. van Ramesdonk, J. W. Verhoeven, F. J. Steemers, E. G. Kerver, W. Verboom, D. N. Reinhoudt, *Chem Eur J* **1998**, *4*, 2315-2323.

[31] Z. Molphy, A. Prisecaru, C. Slator, N. Barron, M. McCann, J. Colleran, D. Chandran, N. Gathergood, A. Kellett, *Inorg Chem* **2014**, *53*, 5392-5404.

[32] H. Xu, K. C. Zheng, H. Deng, L. J. Lin, Q. L. Zhang, L. N. Ji, *New J Chem* **2003**, *27*, 1255-1263.

[33] R. A. Krause, K. Krause, *Inorg Chem* **1982**, *21*, 1714-1720.

[34] C. H. Chien, S. Fujita, S. Yamoto, T. Hara, T. Yamagata, M. Watanabe, K. Mashima, *Dalton Trans* **2008**, 916-923.

[35] K. A. Maghacut, A. B. Wood, W. J. Boyko, T. J. Dudley, J. J. Paul, *Polyhedron* **2014**, *67*, 329-337.

[36] S. P. Pitre, C. D. McTiernan, W. Vine, R. DiPucchio, M. Grenier, J. C. Scaiano, *Sci Rep* **2015**, *5*, 16397.

[37] A. Bahreman, J. A. Cuello-Garibo, S. Bonnet, *Dalton Trans* **2014**, *43*, 4494-4505.